

Modified Gravity: Cosmology without dark matter or a cosmological constant

J. W. Moffat^{1,2} and V. T. Toth¹

¹*Perimeter Institute for Theoretical Physics, Waterloo, Ontario N2L 2Y5, Canada*

²*Department of Physics, University of Waterloo, Waterloo, Ontario N2L 3G1, Canada*

Accepted 2099 December 31. Received 2099 December 31; in original form 2099 December 31

ABSTRACT

We explore the cosmological consequences of Modified Gravity (MOG), and find that it provides, using a minimal number of parameters, good fits to data, including CMB temperature anisotropy, galaxy mass power spectrum, and supernova luminosity-distance observations. The MOG cosmology is flat and predicts an age of the universe of ~ 34 billion years.

Key words: cosmology:theory – large-scale structure of Universe – gravitation.

1 INTRODUCTION

The preferred model of cosmology today, the Λ CDM model, provides an excellent fit to cosmological observations, but at a substantial cost: according to this model, *about 96% of the universe is either invisible or undetectable, or possibly both*. This fact provides a strong incentive to seek alternative explanations that can account for cosmological observations without resorting to dark matter or a cosmological constant.

For gravitational theories designed to challenge the Λ CDM model, the bar is set increasingly higher by recent discoveries. Not only do such theories have to explain successfully the velocity dispersions, rotational curves, and gravitational lensing of galaxies and galaxy clusters, the theories must also be in accord with cosmological observations, notably the acoustic power spectrum of the cosmic microwave background (CMB), the mass power spectrum of galaxies, and the recent observation of the anomalous luminosity-distance relationship of high- z supernovae, which is seen as evidence for “dark energy”.

Modified Gravity (MOG) (Moffat 2006) has been used successfully to account for galaxy cluster masses (Brownstein & Moffat 2006a), the rotation curves of galaxies (Brownstein & Moffat 2006b), velocity dispersions of satellite galaxies (Moffat & Toth 2007b), and globular clusters (Moffat & Toth 2007a). It was also used to offer an explanation for the Bullet Cluster (Brownstein & Moffat 2007) without resorting to cold dark matter.

Remarkably, MOG also meets the challenge posed by cosmological observations. In this paper, it is demonstrated that MOG produces an acoustic power spectrum, a mass power spectrum, and a luminosity-distance relationship that

are in good agreement with observations, and require no dark matter and no cosmological constant.

In the arguments presented here, we rely on simplified analytical calculations. We are not advocating these as substitutes for an accurate numerical analysis. However, a thorough numerical analysis requires significant time and resources; before these are committed, it is useful to be able to demonstrate if a theory is viable, and if the additional effort is warranted.

In the next section, we review the key features of MOG. This is followed by sections presenting detailed calculations for the luminosity-distance relationship of high- z supernovae, the acoustic power spectrum of the CMB, and the galaxy mass power spectrum. A concluding section summarizes our results and maps out future steps.

2 MODIFIED GRAVITY THEORY

Modified Gravity (MOG) is a fully relativistic theory of gravitation that is derived from a relativistic action principle (Moffat 2006) involving scalar, tensor, and vector fields. MOG has evolved as a result of investigations of Nonsymmetric Gravity Theory (NGT, Moffat (1995)), and most recently, it has taken the form of Scalar-Tensor-Vector Gravity (STVG, Moffat (2006)). In the weak field approximation, STVG, NGT, and Metric-Skew-Tensor Gravity (MSTG, Moffat (2005)) produce similar results.

2.1 Scalar-Tensor-Vector Gravity

Our modified gravity theory is based on postulating the existence of a massive vector field, ϕ_μ . The choice of a massive vector field is motivated by our desire to introduce a *repulsive* modification of the law of gravitation at short range. The vector field is coupled universally to matter. The theory, therefore, has three constants: in addition to the gravitational constant G , we must also consider the coupling constant ω that determines the coupling strength between the ϕ_μ field and matter, and a further constant μ that arises as a result of considering a vector field of non-zero mass, and controls the coupling range. In the most general case, these constants must be allowed to run, resulting in the following action (we assume that the speed of light, $c = 1$):

$$S = S_G + S_\phi + S_S + S_M, \quad (1)$$

where

$$S_G = \frac{1}{16\pi} \int \frac{1}{G} (R + 2\Lambda) \sqrt{-g} d^4x, \quad (2)$$

$$S_\phi = - \int \omega \left[\frac{1}{4} B^{\mu\nu} B_{\mu\nu} + V(\phi) \right] \sqrt{-g} d^4x, \quad (3)$$

$$S_S = \int \frac{1}{G} \left[\frac{1}{2} g^{\mu\nu} \left(\frac{G_{;\mu} G_{;\nu}}{G^2} + \frac{\mu_{;\mu} \mu_{;\nu}}{\mu^2} + \omega_{;\mu} \omega_{;\nu} \right) - \frac{V(G)}{G^2} - \frac{V(\mu)}{\mu^2} - V(\omega) \right] \sqrt{-g} d^4x, \quad (4)$$

where S_M is the “matter” action, $V(\phi)$ is the potential associated with ϕ_μ , $B_{\mu\nu} = \partial_{[\mu} \phi_{\nu]}$, while $V(G)$, $V(\omega)$, and $V(\mu)$ denote the three potentials associated with the three scalar fields. The semicolon is used to denote covariant differentiation, square brackets indicate antisymmetrization of indices ($X_{[\mu\nu]} = X_{\mu\nu} - X_{\nu\mu}$), while the symbols R , Λ , and g represent the Ricci-scalar, the cosmological constant, and the metric tensor, respectively. The theory does not prescribe the form of the potential functions $V(\phi)$, $V(G)$, $V(\mu)$, and $V(\omega)$.

The energy-momentum tensor is defined as

$$T_{\mu\nu} = T_{M\mu\nu} + T_{\phi\mu\nu} + T_{S\mu\nu}, \quad (5)$$

where

$$T_{X\mu\nu} = - \frac{2}{\sqrt{-g}} \frac{\delta S_X}{\delta g^{\mu\nu}}, \quad (X = [M, \phi, S]). \quad (6)$$

The field equations can be obtained from the variation of $g^{\mu\nu}$:

$$G_{\mu\nu} - g_{\mu\nu} \Lambda + Q_{\mu\nu} = 8\pi G T_{\mu\nu}, \quad (7)$$

where

$$Q_{\mu\nu} = G (g^{\alpha\beta} \Theta_{;\alpha\beta} g_{\mu\nu} - \Theta_{;\mu\nu}), \quad (8)$$

and $\Theta(x) = G^{-1}(x)$.

Our cosmological considerations are based on a homogeneous and isotropic universe with a Friedmann-Lemaître-Robertson-Walker (FLRW) background metric with line element

$$ds^2 = dt^2 - a^2(t) \left(\frac{dr^2}{1 - kr^2} + r^2 d\Omega^2 \right), \quad (9)$$

where $d\Omega^2 = d\theta^2 + \sin^2 \theta d\phi^2$ and $k = -1, 0, 1$ for open, flat, and closed universes, respectively. We use the energy-momentum tensor of a perfect fluid

$$T^{\mu\nu} = (\rho + p) u^\mu u^\nu - p g^{\mu\nu}, \quad (10)$$

where $u^\mu = dx^\mu/ds$ and the density ρ and pressure p include contributions from matter, the vector field ϕ^μ and the scalar fields G , ω , and μ .

Due to the symmetries of the FLRW background space-time, we have $\phi_0 \neq 0$, $\phi_i = 0$, and $B_{\mu\nu} = 0$.

The MOG Friedmann equations read (Moffat 2006, 2007)

$$\left(\frac{\dot{a}}{a} \right)^2 + \frac{k}{a^2} = \frac{8\pi G \rho}{3} + f(t) + \frac{\Lambda}{3}, \quad (11)$$

$$\frac{\ddot{a}}{a} = - \frac{4\pi G}{3} (\rho + 3p) + h(t) + \frac{\Lambda}{3}, \quad (12)$$

where

$$f(t) = \frac{\dot{a}}{a} \frac{\dot{G}}{G}, \quad (13)$$

and¹

$$h(t) = \frac{1}{2} \left(\frac{\ddot{G}}{G} - 2 \frac{\dot{G}^2}{G^2} + \frac{\dot{a}}{a} \frac{\dot{G}}{G} \right). \quad (14)$$

From (11) we obtain

$$\dot{\rho} + 3 \frac{d \ln a}{dt} (\rho + p) + \frac{\dot{G}}{G} \rho + \mathcal{I} = 0, \quad (15)$$

where

$$\mathcal{I} = \frac{3}{8\pi G a} (2\dot{a}f + a\dot{f} - 2\dot{a}h). \quad (16)$$

2.2 Weak field approximation

In the weak field, spherically symmetric case MOG yields the gravitational acceleration law (Moffat 2006, 2007):

$$a(r) = - \frac{G_\infty M}{r^2} \left[1 - \frac{\alpha}{1 + \alpha} (1 + \mu r) e^{-\mu r} \right], \quad (17)$$

where α and μ are constants of the theory (note that the theory allows these constants to be running; however, in the present work, we make little use of this fact), and the coupling constant G_∞ is related to Newton’s constant of gravitation G_N by $G_\infty = (1 + \alpha)G_N$.

Although at first sight, Eq. (17) may seem applicable to point masses only, it is in fact applicable to extended distributions of matter, as it can be derived from the MOG Poisson equation (Brownstein & Moffat (2007); see also Sec. 5.2 below.)

This acceleration law describes a theory of gravity, characterized by the gravitational constant G_∞ , and modified at short range by a *repulsive* Yukawa-force. At distances much larger than μ^{-1} , the Yukawa-force vanishes, and we obtain Newton’s theory of gravitation with G_∞ as the gravitational

¹ The expressions for $h(t)$ and \mathcal{I} presented here differ from their form published by Moffat (2006, 2007); this is a result of a recalculation.

constant. At shorter distances, the gravitational force can be described by the effective gravitational constant

$$G(r) = G_\infty \left[1 - \frac{\alpha}{1 + \alpha} (1 + \mu r) e^{-\mu r} \right]. \quad (18)$$

In all cases to date when the predictions of MOG were compared to observational data, the value of μ was $(1 \text{ pc})^{-1}$ or less, equivalent to a Yukawa-force λ -parameter greater than $10^{16} - 10^{17} \text{ m}$. The corresponding value of $\alpha/(1 + \alpha)$ is between ~ 0.8 and ~ 0.95 . These values are consistent with observational constraints on the inverse-square law (Fischbach & Talmadge 1998; Adelberger et al. 2003).

The distance dependence of the effective gravitational constant deserves further remarks. First, we note that as we move from a fully relativistic field theory to a 3+1-dimensional weak field approximation, the meaning of G changes: it no longer represents the local value of a 4-dimensional field, but rather, it now plays the role of the coupling constant of an “action-at-a-distance” type force between distant interacting bodies. Second, the effective value of G in the weak field approximation is a result of the interaction between the fields in the full theory, most notably the ϕ and μ fields, in addition to G itself. Lastly, we need to mention that the distance dependence of G by no means precludes the notion of an homogeneous and isotropic universe: in this sense, the distance dependence of G is no more significant than the r^{-2} distance-dependence in Newton’s gravitational force law, and in a homogeneous and isotropic universe, all distance dependencies cancel out exactly, without introducing a preferred spatial direction.

2.3 Cosmological considerations

We begin with the MOG Friedmann equations from Section 2.1. We assume a flat universe ($k = 0$) with no cosmological constant ($\Lambda = 0$). Furthermore, we assume that the time dependence of the gravitational constant is negligible, $\dot{G} \simeq 0$. We obtain the Friedmann equations:

$$H^2 \equiv \left(\frac{\dot{a}}{a} \right)^2 = \frac{8\pi G \rho}{3}, \quad (19)$$

$$-H^2 q \equiv \frac{\ddot{a}}{a} = -\frac{4\pi G}{3}(\rho + 3p), \quad (20)$$

defining an Einstein-de Sitter universe. From (15), we obtain the energy conservation equation

$$\dot{\rho} + 3\frac{d \ln a}{dt}(\rho + p) = 0, \quad (21)$$

that, in the matter-dominated universe ($p = 0$), yields

$$\rho \propto a^{-3}. \quad (22)$$

When the strength of the gravitational interaction is low, the value of the gravitational constant can be well approximated by the non-relativistic effective value (18) developed in the previous section. At distances much greater than μ^{-1} , $G(r) = G_\infty$. The Friedmann equations then read²,

$$\Omega_M = \frac{8\pi G_\infty \rho}{3H^2} = 1, \quad (23)$$

$$q = \frac{\Omega_M}{2}(1 + 3w), \quad (24)$$

where $w = p/\rho$. As the density of the universe is known experimentally, the above equation determines G_∞ . Assuming only “visible” matter (i.e., baryons and, possibly, neutrinos) amounting to $\sim 5\%$ of the critical density calculated using G_N , we get

$$G_\infty \simeq 20G_N. \quad (25)$$

This, in turn, defines the value of α :

$$\alpha = \frac{G_\infty}{G_N} - 1 \simeq 19. \quad (26)$$

MOG presently does not prescribe a value for the constant μ . However, in the cosmological context, an obvious choice presents itself:

$$\mu = \frac{1}{a_0}, \quad (27)$$

where we fix a_0 to be the horizon distance.

The most profound consequence of MOG is that the *apparent* values of Ω_M and q in the Friedmann equations will differ from the values one would expect in a flat cosmology. As one performs cosmological measurements using a *locally* obtained value of G , one will observe, using (23) and (24):

$$\Omega'_M = \frac{G}{G_\infty} \Omega_M = \frac{G}{G_\infty}, \quad (28)$$

and

$$q' = \frac{G}{G_\infty} q. \quad (29)$$

How can one reconcile the apparent inconsistency of (28) with the first Friedmann equation (19), for clearly, $1 \neq \Omega'_M$? However, this is a result of the fact that Ω'_M represents an observed quantity based on the *screened* value of the gravitational constant, whereas the geometry of the universe is determined by the constant’s “bare” value, G_∞ . Therefore, the first Friedmann equation (19) can be correctly written as:

$$1 = \Omega'_M + \Omega_\Delta, \quad (30)$$

where

$$\Omega_\Delta = \frac{G_\infty - G(r)}{G_\infty}. \quad (31)$$

On the other hand, the observed value of the deceleration parameter, q , is based on Ω'_M alone, hence the second Friedmann equation (20) will remain in the form of (29).

preferred direction is introduced, as indicated at the end of the previous section. This assertion can also be verified by explicitly calculating the MOG gravitational force inside a spherically symmetric homogeneous distribution of matter, and taking the radius of the sphere to infinity.

² Indeed, G_∞ is the only possible value that can appear in the Friedmann equations, otherwise, through distance dependence, a

2.4 The age of the universe

Calculating the age of an Einstein-de Sitter universe from the first Friedmann equation (19) gives $2/3H_0$, an unacceptably small value given the best known value of the Hubble constant, $H_0 \simeq 71$ km/s/Mpc. However, the apparent age of the MOG universe has to be calculated using the observed value of the gravitational constant.

By (23), we have

$$\frac{8\pi G_\infty \rho_0}{3} = H_0^2. \quad (32)$$

We take this equation to represent the universe in the kinematic limit, and as such, we expect it to correctly describe purely geometric measurements, such as measurements of Hubble's constant. In this limit, the age of the Universe is $2/3H_0$.

A co-moving observer may, however, calculate elapsed time differently: applying the screened value of the gravitational constant from the dynamical theory, rather than its bare value. Instead of writing the first Friedmann equation (19) using G_∞ , this observer may use the effective value G of the gravitational constant. Then, using the conservation law (21),

$$\left(\frac{\dot{a}}{a}\right)^2 = \frac{8\pi G\rho}{3} = \left(\frac{8\pi G_\infty \rho_0}{3}\right) \frac{G}{G_\infty} \frac{\rho}{\rho_0} = H_0^2 \frac{G}{G_\infty} \frac{a_0^3}{a^3}. \quad (33)$$

Since G is known as a function of r (18), which, in turn, can be expressed as a function of a (see Eq. 42 below), we obtain

$$G(a) = G_\infty \left\{ 1 - \frac{\alpha}{1+\alpha} [1 + \mu(a_0 - \sqrt{a_0 a})] e^{-\mu(a_0 - \sqrt{a_0 a})} \right\}, \quad (34)$$

and Eq. (33) can be solved by direct integration:

$$\sqrt{\frac{G_\infty}{H_0^2 a_0^3}} \int_0^{a_0} \sqrt{\frac{a}{G(a)}} da = t_0, \quad (35)$$

where t_0 is the age of the universe. Using $\alpha = 19$, we obtain

$$t_0 \simeq 3.4 \times 10^{10} \text{ years}. \quad (36)$$

Eq. 35 can also be written as a function of z , allowing us to calculate the time between various events characterized by redshift. For instance, the time from the Big Bang to recombination ($z \simeq 1100$) is

$$t_{\text{rec}} \simeq 460,000 \text{ years}. \quad (37)$$

3 MOG AND THE LUMINOSITY-DISTANCE RELATIONSHIP OF HIGH- Z SUPERNOVAE

Type Ia supernovae are excellent standard candles for astronomy. The physics of these massive explosions is believed to be well understood, and it determines their peak luminosity. The distance to these events can be calculated from their redshift; knowing the distance and their absolute luminosity, their apparent luminosity can be computed.

The difference $\mu(z)$ between the absolute and apparent luminosity of a distant object can be calculated as a function of the redshift z , Hubble constant H , and cosmic deceleration q as (Weinberg 1972):

$$\mu(z) = 25 - 5 \log_{10} H + 5 \log_{10}(cz) + 1.086(1 - q)z + \dots \quad (38)$$

Even after corrections for astrophysical dimming are applied, supernova observations are not consistent with the $q = 0.5$ value of an Einstein-de Sitter universe. The data are consistent, however, with solutions that predict $q \simeq 0$, such as the predictions of the Λ CDM concordance model.

3.1 Redshift and Cosmic Deceleration in Modified Gravity

As discussed in Section 2.3, MOG predicts a much reduced *apparent* value of the deceleration parameter q . This is a result of the fact that the effective gravitational constant, G , is a screened value of G_∞ at short distances. Here, “short” means less than several times the reciprocal of the MOG parameter μ ; using the natural choice of $\mu = a_0^{-1}$, the prediction is that $q \ll 0.5$ up to the horizon distance, i.e., $r < a_0$.

As the Yukawa-term in the MOG weak-field approximation (17) depends on the distance r , we need a formula capturing the relationship between r and a . From the FLRW metric (9), setting the line element ds and $d\Omega$ both to zero, we obtain

$$dt^2 = a^2(t) dr^2, \quad (39)$$

which yields

$$\int \frac{1}{a\dot{a}} da = r. \quad (40)$$

As we are free to choose our units for r and a , we are only interested in the relationship between these quantities up to a proportionality factor. From the Einstein-de Sitter solution, we have $a \propto t^{2/3}$, or

$$a\dot{a} \propto t^{1/3} \propto \sqrt{a}, \quad (41)$$

hence, with an appropriate choice of units, we get

$$r = a_0 - \sqrt{a_0} \sqrt{a}. \quad (42)$$

Cosmological distances are often measured using the redshift parameter z , defined as

$$z = \frac{a_0 - a}{a}. \quad (43)$$

This, in turn, allows us to rewrite the effective gravitational constant (18) as a function of z :

$$G(z) = G_\infty \left\{ 1 - \frac{\alpha}{(1+\alpha)} \frac{1 + \mu a_0 (1 - (z+1)^{-1/2})}{\exp(\mu a_0 [1 - (z+1)^{-1/2}])} \right\}. \quad (44)$$

We note that the limit of $G(z)$ as $z \rightarrow \infty$ is *not* G_∞ :

$$\lim_{z \rightarrow \infty} G(z) = G_\infty \left[1 - \frac{\alpha}{1+\alpha} (1 + \mu a_0) e^{-\mu a_0} \right]. \quad (45)$$

This is a consequence of the fact that in a flat universe, the horizon is not at spatial infinity but at a finite distance from the observer. Using $\alpha = 19$ and $\mu = a_0^{-1}$, this expression evaluates to

$$\bar{G} = \lim_{z \rightarrow \infty} G(z) \simeq 0.3 G_\infty. \quad (46)$$

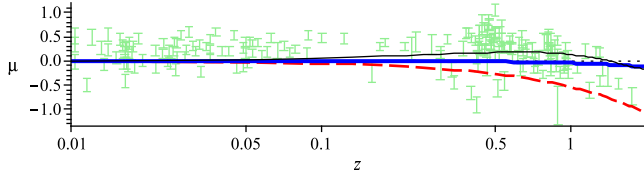


Figure 1. Type Ia supernova luminosity-redshift data (Riess et al. 2004), in comparison with several models. No astrophysical dimming was applied. The horizontal axis corresponds with the $q = 0$ empty universe. Dashed (red) line is an Einstein de-Sitter universe with $\Omega_M = 1$, $q = 0.5$. Thin black line is the Λ CDM model, represented here by a simplistic fitting formula, while the thick (blue) line is the MOG prediction.

3.2 Comparison with observations

The result of these calculations is presented in Figure 1. To compare MOG’s predictions with actual data, we used the Type Ia supernova data set compiled by Riess et al. (2004).

The most significant difference between the MOG and Λ CDM predictions is that MOG can fit supernova observations without being “locked in” to predict cosmic acceleration at later epochs. Indeed, in the absence of a cosmological constant, MOG may only predict an accelerating expansion if $\dot{G} \neq 0$ and $h(t) > 0$ (14).

As a result, a notable difference between the MOG and Λ CDM predictions can be seen at high values of z . At first sight, the data seem to favor an accelerating solution, as the data points tend to cluster above the $q = 0$ axis. Note, however, that we made no attempt to account for astrophysical dimming (see, for instance, Goobar et al. (2002)), which would also manifest itself as an apparent acceleration.

3.3 Discussion

From Figure 1, it is clear that both MOG and Λ CDM provide a model that is superior to the “naive” Einstein-de Sitter solution with $\Omega_M = 1$ and $q = 0.5$. Although the two models are qualitatively different (one predicts acceleration, whereas the other does not), in practice, this difference is only observable at high values of z , where there is more uncertainty in the data and their interpretation, due, e.g., to astrophysical dimming.

For these reasons, while we can state with confidence that MOG is in good agreement with supernova observations, it is unclear at present if observations of this nature can unambiguously distinguish between MOG and Λ CDM.

4 MOG AND THE CMB

The cosmic microwave background (CMB) is highly isotropic, showing only small temperature fluctuations as a function of sky direction. These fluctuations are not uniformly random; they show a distinct dependence on angular size, as has been demonstrated by the measurements of the Boomerang experiment (Jones et al. 2006) and the Wilkinson Microwave Anisotropy Probe (WMAP) (Spergel et al. 2007).

The angular temperature fluctuations of the CMB can be calculated in a variety of ways. The preferred method is to use numerical software, such as CMBFAST (Seljak & Zaldarriaga 1996). Unfortunately, such software packages cannot easily be adapted for use with MOG. Instead, at the present time we opt to use the excellent semi-analytical approximation developed by Mukhanov (2005), which, while not as accurate as numerical software, lends itself more easily to nontrivial modifications, as the physics remains up front and evident in the equations.

4.1 Semi-analytical estimation of CMB anisotropies

Mukhanov (2005) calculates the correlation function $C(l)$, where l is the multipole number, of the acoustic spectrum of the CMB using the solution

$$\frac{C(l)}{[C(l)]_{\text{low } l}} = \frac{100}{9}(O + N), \quad (47)$$

where $l \gg 1$, O denotes the oscillating part of the spectrum, while the non-oscillating part is written as the sum of three parts:

$$N = N_1 + N_2 + N_3. \quad (48)$$

These, in turn, are expressed as

$$N_1 = 0.063\xi^2 \frac{[P - 0.22(l/l_f)^{0.3} - 2.6]^2}{1 + 0.65(l/l_f)^{1.4}} e^{-(l/l_f)^2}, \quad (49)$$

$$N_2 = \frac{0.037}{(1 + \xi)^{1/2}} \frac{[P - 0.22(l/l_s)^{0.3} + 1.7]^2}{1 + 0.65(l/l_s)^{1.4}} e^{-(l/l_s)^2}, \quad (50)$$

$$N_3 = \frac{0.033}{(1 + \xi)^{3/2}} \frac{[P - 0.5(l/l_s)^{0.55} + 2.2]^2}{1 + 2(l/l_s)^2} e^{-(l/l_s)^2}. \quad (51)$$

The oscillating part of the spectrum is written as

$$O = \sqrt{\frac{\pi}{\rho l}} \left[A_1 \cos\left(\rho l + \frac{\pi}{4}\right) + A_2 \cos\left(2\rho l + \frac{\pi}{4}\right) \right] e^{-(l/l_s)^2}, \quad (52)$$

where

$$A_1 = 0.1\xi \frac{(P - 0.78)^2 - 4.3}{(1 + \xi)^{1/4}} e^{\frac{1}{2}(l_s^{-2} - l_f^{-2})l^2}, \quad (53)$$

and

$$A_2 = 0.14 \frac{(0.5 + 0.36P)^2}{(1 + \xi)^{1/2}}. \quad (54)$$

The parameters that occur in these expressions are as follows. First, the baryon density parameter:

$$\xi = 17 \left(\Omega_b h_{75}^2 \right), \quad (55)$$

where $\Omega_b \simeq 0.035$ is the baryon content of the universe at present relative to the critical density, and $h_{75} = H/(75 \text{ km/s/Mpc})$. The growth term of the transfer function is represented by

$$P = \ln \frac{\Omega_m^{-0.09} l}{200 \sqrt{\Omega_m h_{75}^2}}, \quad (56)$$

where $\Omega_m \simeq 0.3$ is the total matter content (baryonic matter, neutrinos, and cold dark matter). The free-streaming and Silk damping scales are determined, respectively, by

$$l_f = 1300 \left[1 + 7.8 \times 10^{-2} (\Omega_m h_{75}^2)^{-1} \right]^{1/2} \Omega_m^{0.09}, \quad (57)$$

$$l_s = \frac{0.7 l_f}{\sqrt{\frac{1+0.56\xi}{1+\xi} + \frac{0.8}{\xi(1+\xi)} \frac{(\Omega_m h_{75}^2)^{1/2}}{\left[1 + \left(1 + \frac{100}{7.8} \Omega_m h_{75}^2\right)^{-1/2}\right]^2}}}. \quad (58)$$

Lastly, the location of the acoustic peaks is determined by the parameter³

$$\bar{\rho} = 0.015(1 + 0.13\xi)^{-1} (\Omega_m h_{75}^{3.1})^{0.16}. \quad (59)$$

4.2 The MOG CMB spectrum

The semi-analytical approximation presented in the previous section can be adapted to the MOG case by making three important observations.

First, in all expressions involving the value of Ω_m , we need to use $\bar{\Omega}_M = \bar{G}/G_\infty \simeq 0.3$ (28, 46).

Second, we note that the role of Ω_Λ is taken over by Ω_Δ in (31), as the value that “completes” Ω to satisfy the Einstein-de Sitter cosmology.

Third, we notice that the value of Ω_b in (55) *does not depend on the effective value of the gravitational constant*, as this value is a function of the speed of sound, which depends on the (baryonic) matter density, regardless of gravitation. In other words, $\Omega_b \simeq 0.035$ is calculated using Newton’s gravitational constant.

After we modify Mukhanov’s semi-analytical formulation by taking these considerations into account, we obtain the fit to the acoustic power spectrum shown in Figure 2.

4.3 Discussion

As figure 2 demonstrates, to the extent that Mukhanov’s formulation is applicable to MOG, the theory achieves excellent agreement with the observed acoustic spectrum. We wish to emphasize that this result was obtained with no fine-tuning whatsoever. The value of the MOG constant α was obtained by postulating an Einstein-de Sitter universe; the MOG constant μ was assumed to take on the “cosmological” value a_0^{-1} . Critically, the value of $\bar{\Omega}_M \simeq 0.3$ is a consequence of the theory, not a value that was put in by hand.

5 MOG AND THE MASS POWER SPECTRUM

The distribution of mass in the universe is not uniform. Due to gravitational self-attraction, matter tends to “clump” into ever denser concentrations, leaving large voids in between. In the early universe, this process is counteracted by pressure. The process is further complicated by the fact that

³ Note that we slightly adjusted the coefficients of (57) and (59), which improved the fit noticeably, while remaining fully consistent with Mukhanov’s derivation.

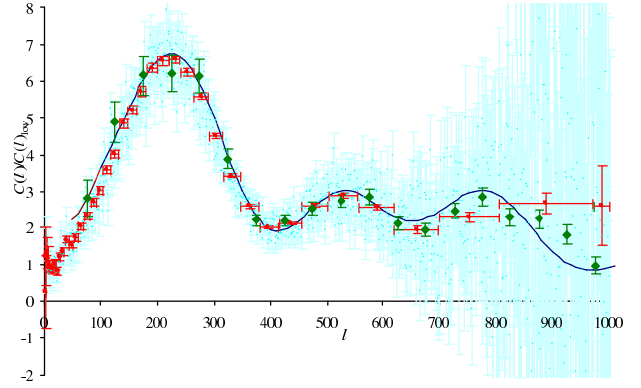


Figure 2. MOG and the acoustic power spectrum. Calculated using $\bar{\Omega}_M = 0.3$, $\Omega_b = 0.035$, $H_0 = 71$ km/s/Mpc. Also shown are the raw WMAP 3-year data set (light blue), binned averages with horizontal and vertical error bars provided by the WMAP project (red), and data from the Boomerang experiment (green).

in the early universe, the energy density of radiation was comparable to that of matter.

5.1 Density fluctuations in Newtonian gravity

To first order, this process can be investigated using perturbation theory. Taking an arbitrary initial distribution, one can proceed to introduce small perturbations in the density, velocity, and acceleration fields. These lead to a second-order differential equation for the density perturbation that can be solved analytically or numerically. This yields the *transfer function*, which determines how an initial density distribution evolves as a function of time in the presence of small perturbations.

5.1.1 Newtonian theory of small fluctuations

In order to see how this theory can be developed for MOG, we must first review how the density perturbation equation is derived in the Newtonian case. Our treatment follows closely the approach presented by Weinberg (1972). We begin with three equations: the continuity equation, the Euler equation, and the Poisson equation.

$$\frac{\partial \rho}{\partial t} + \nabla \cdot (\rho \mathbf{v}) = 0, \quad (60a)$$

$$\frac{\partial \mathbf{v}}{\partial t} + (\mathbf{v} \cdot \nabla) \mathbf{v} = -\frac{1}{\rho} \nabla p + \mathbf{g}, \quad (60b)$$

$$\nabla \cdot \mathbf{g} = -4\pi G \rho. \quad (60c)$$

We begin with perturbing ρ , p , \mathbf{v} and \mathbf{g} . Spelled out in full, we get:

$$\frac{\partial(\rho + \delta\rho)}{\partial t} + \nabla \cdot [(\rho + \delta\rho)(\mathbf{v} + \delta\mathbf{v})] = 0, \quad (61a)$$

$$\frac{\partial(\mathbf{v} + \delta\mathbf{v})}{\partial t} + [(\mathbf{v} + \delta\mathbf{v}) \cdot \nabla](\mathbf{v} + \delta\mathbf{v}) = \quad (61b)$$

$$-\frac{1}{\rho + \delta\rho}\nabla(p + \delta p) + \mathbf{g} + \delta\mathbf{g},$$

$$\nabla \cdot (\mathbf{g} + \delta\mathbf{g}) = -4\pi G(\rho + \delta\rho). \quad (61c)$$

Subtracting the original set of equations from the new set, using $1/(\rho + \delta\rho) = (\rho - \delta\rho)/[\rho^2 - (\delta\rho)^2] = 1/\rho - \delta\rho/\rho^2$, and eliminating second-order terms, we obtain

$$\frac{\partial\delta\rho}{\partial t} + \nabla \cdot (\delta\rho\mathbf{v} + \rho\delta\mathbf{v}) = 0, \quad (62a)$$

$$\frac{\partial\delta\mathbf{v}}{\partial t} + (\mathbf{v} \cdot \nabla)\delta\mathbf{v} + (\delta\mathbf{v} \cdot \nabla)\mathbf{v} = \frac{\delta\rho}{\rho^2}\nabla p - \frac{1}{\rho}\nabla\delta p + \delta\mathbf{g}, \quad (62b)$$

$$\nabla \cdot \delta\mathbf{g} = -4\pi G\delta\rho. \quad (62c)$$

A further substitution can be made by observing that $\delta p = (\delta p/\delta\rho)\delta\rho = c_s^2\delta\rho$ where $c_s = (\partial p/\partial\rho)_{\text{adiabatic}}$ is the speed of sound. We can also eliminate terms by observing that the original (unperturbed) state is spatially homogeneous, hence $\nabla\rho = \nabla p = 0$:

$$\frac{\partial\delta\rho}{\partial t} + \mathbf{v} \cdot \nabla\delta\rho + \delta\rho\nabla \cdot \mathbf{v} + \rho\nabla \cdot \delta\mathbf{v} = 0, \quad (63a)$$

$$\frac{\partial\delta\mathbf{v}}{\partial t} + (\mathbf{v} \cdot \nabla)\delta\mathbf{v} + (\delta\mathbf{v} \cdot \nabla)\mathbf{v} = -\frac{c_s^2}{\rho}\nabla\delta\rho + \delta\mathbf{g}, \quad (63b)$$

$$\nabla \cdot \delta\mathbf{g} = -4\pi G\delta\rho. \quad (63c)$$

Now we note that $\mathbf{v} = H\mathbf{x}$, hence

$$\nabla \cdot \mathbf{v} = H\nabla \cdot \mathbf{x} = 3H,$$

$$(\delta\mathbf{v} \cdot \nabla)\mathbf{v} = (\delta\mathbf{v} \cdot \nabla)(H\mathbf{x}) = H(\delta\mathbf{v} \cdot \nabla)\mathbf{x} = H\delta\mathbf{v}.$$

Therefore,

$$\frac{\partial\delta\rho}{\partial t} + \mathbf{v} \cdot \nabla\delta\rho + 3H\delta\rho + \rho\nabla \cdot \delta\mathbf{v} = 0, \quad (64a)$$

$$\frac{\partial\delta\mathbf{v}}{\partial t} + (\mathbf{v} \cdot \nabla)\delta\mathbf{v} + H\delta\mathbf{v} = -\frac{c_s^2}{\rho}\nabla\delta\rho + \delta\mathbf{g}, \quad (64b)$$

$$\nabla \cdot \delta\mathbf{g} = -4\pi G\delta\rho. \quad (64c)$$

The next step is a change of spatial coordinates to coordinates comoving with the Hubble flow:

$$\mathbf{x} = a(t)\mathbf{q}.$$

This means

$$\left(\frac{\partial}{\partial t}\right)_{\mathbf{q}} = \left(\frac{\partial}{\partial t}\right)_{\mathbf{x}} + \mathbf{v}\nabla_{\mathbf{x}}, \text{ and}$$

$$\nabla_{\mathbf{q}} = a\nabla_{\mathbf{x}}.$$

After this change of coordinates, our system of equations becomes

$$\frac{\partial\delta\rho}{\partial t} + 3H\delta\rho + \frac{1}{a}\rho\nabla \cdot \delta\mathbf{v} = 0, \quad (65a)$$

$$\frac{\partial\delta\mathbf{v}}{\partial t} + H\delta\mathbf{v} = -\frac{c_s^2}{a\rho}\nabla\delta\rho + \delta\mathbf{g}, \quad (65b)$$

$$\nabla \cdot \delta\mathbf{g} = -4\pi aG\delta\rho. \quad (65c)$$

Now is the time to introduce the fractional amplitude $\delta = \delta\rho/\rho$. Dividing (65a) with ρ , we get

$$\dot{\delta} + \frac{\dot{\rho}}{\rho}\delta + 3H\delta + \frac{1}{a}\nabla \cdot \delta\mathbf{v} = 0. \quad (66)$$

However, since $\rho = \rho_0 a_0^3/a^3$, and hence $\dot{\rho}/\rho = -3\dot{a}/a$, the second and third terms cancel, to give

$$-a\dot{\delta} = \nabla\delta\mathbf{v}. \quad (67)$$

Taking the gradient of (65b) and using (65c) to express $\nabla \cdot \delta\mathbf{g}$, we get

$$\frac{\partial}{\partial t}(-a\dot{\delta}) + H(-a\dot{\delta}) = -\frac{c_s^2}{a}\nabla^2\delta - 4\pi Ga\rho\delta. \quad (68)$$

Spelling out the derivatives, and dividing both sides with a , we obtain

$$\ddot{\delta} + 2H\dot{\delta} - \frac{c_s^2}{a^2}\nabla^2\delta - 4\pi G\rho\delta = 0. \quad (69)$$

For every Fourier mode $\delta = \delta_{\mathbf{k}}(t)e^{i\mathbf{k}\cdot\mathbf{q}}$ (such that $\nabla^2\delta = -k^2\delta$), this gives

$$\ddot{\delta}_{\mathbf{k}} + 2H\dot{\delta}_{\mathbf{k}} + \left(\frac{c_s^2 k^2}{a^2} - 4\pi G\rho\right)\delta_{\mathbf{k}} = 0. \quad (70)$$

The quantity k/a is called the co-moving wave number.

If k is large, solutions to (70) are dominated by an oscillatory term; for small k , a growth term predominates.

A solution to (70) tells us how a power spectrum evolves over time, as a function of the wave number; it does not specify the initial power spectrum. For this reason, solutions to (70) are typically written in the form of a transfer function

$$T(k) = \frac{\delta_{\mathbf{k}}(z=0)\delta_0(z=\infty)}{\delta_{\mathbf{k}}(z=\infty)\delta_0(z=0)}. \quad (71)$$

If the initial power spectrum and the transfer function are known, the power spectrum at a later time can be calculated (without accounting for small effects) as

$$P(k) = T^2(k)P_0(k). \quad (72)$$

$P(k)$ is a dimensioned quantity. It is possible to form the dimensionless power spectrum

$$\Delta^2(k) = Ak^3T^2(k)P_0(k), \quad (73)$$

where A is a normalization constant determined by observation. This form often appears in the literature. In the present work, however, we are using $P(k)$, not $\Delta(k)$.

The initial power spectrum is believed to be a scale invariant power spectrum:

$$P_0(k) \propto k^n, \quad (74)$$

where $n \simeq 1$. The best current estimate on n is $n = 0.951^{+0.015}_{-0.019}$ (Spergel et al. 2007).

5.1.2 Analytical approximation

Eq. 70 is not difficult to solve in principle. The solution can be written as the sum of oscillatory and growing terms. The usual physical interpretation is that when pressure is sufficient to counteract gravitational attraction, this mechanism prevents the growth of density fluctuations, and their energy is dissipated instead in the form of sound waves; when the pressure is low, however, the growth term dominates and fluctuations grow. Put into the context of an expanding universe, one can conclude that in the early stages, when

the universe was hot and dense, the oscillatory term had to dominate; later, the growth term took over, the perturbation spectrum “froze”, affected only by uniform growth afterwards.

In practice, several issues complicate the problem. First, the early universe cannot be modeled by matter alone; it contained a mix of matter and radiation (and, possibly, neutrinos and cold dark matter.) To correctly describe this case even using the linear perturbation theory outlined in the previous sections, one needs to resort to a system of coupled differential equations describing the different mediums. Second, if the perturbations are sufficiently strong, linear theory may no longer be valid. Third, other nonlinear effects, including Silk-damping (Padmanabhan 1993), cannot be excluded as their contribution is significant (indeed, Silk damping at higher wave numbers is one of the reasons why a baryon-only cosmological model fails to account for the matter power spectrum.)

Eisenstein & Hu (1998) addressed all these issues when they developed a semi-analytical solution to the baryon transfer function. This solution reportedly yields good results in the full range of $0 \leq \Omega_b \leq 1$. Furthermore, unlike other approximations and numerical software codes, this approach keeps the essential physics transparent, allowing us to adapt the formulation for the MOG case.

Eisenstein & Hu (1998) write the transfer function as the sum of a baryonic term T_b and a cold dark matter term T_c :

$$T(k) = \frac{\Omega_b}{\Omega_m} T_b(k) + \frac{\Omega_c}{\Omega_m} T_c(k), \quad (75)$$

where Ω_c represents the cold dark matter content of the universe relative to the critical density. As we are investigating a cosmology with no cold dark matter, we ignore T_c . The baryonic part of the transfer function departs from the cold dark matter case on scales comparable to, or smaller than, the sound horizon. Consequently, the baryonic transfer function is written as

$$T_b(k) = \left[\frac{\tilde{T}_0(k, 1, 1)}{1 + (ks/5.2)^2} + \frac{\alpha_b e^{-(k/k_{\text{Silk}})^{1.4}}}{1 + (\beta_b/ks)^3} \right] \frac{\sin k\tilde{s}}{k\tilde{s}}, \quad (76)$$

with

$$\tilde{T}_0(k, \alpha_c, \beta_c) = \frac{\ln(e + 1.8\beta_c \bar{q})}{\ln(e + 1.8\beta_c \bar{q}) + C\bar{q}^2}, \quad (77)$$

where

$$C = \frac{14.2}{\alpha_c} + \frac{386}{1 + 69.9\bar{q}^{1.08}}, \quad (78)$$

and

$$\bar{q} = k\Theta_{2.7}^2 (\Omega_m h^2)^{-1}. \quad (79)$$

The sound horizon is calculated as

$$s = \frac{2}{3k_{\text{eq}}} \sqrt{\frac{G}{R_{\text{eq}}}} \ln \frac{\sqrt{1 + R_d} + \sqrt{R_d + R_{\text{eq}}}}{1 + \sqrt{R_{\text{eq}}}}. \quad (80)$$

The scale at the equalization epoch is calculated as

$$k_{\text{eq}} = 7.46 \times 10^{-2} \Omega_m h^2 \Theta_{2.7}^{-2}. \quad (81)$$

The transition from a radiation-dominated to a matter-dominated era happens at the redshift

$$z_{\text{eq}} = 25000 \Omega_m h^2 \Theta_{2.7}^{-4}, \quad (82)$$

while the drag era is defined as

$$z_d = 1291 \frac{(\Omega_m h^2)^{0.251}}{1 + 0.659(\Omega_m h^2)^{0.828}} [1 + b_1(\Omega_m h^2)^{b_2}], \quad (83)$$

where

$$b_1 = 0.313(\Omega_m h^2)^{-0.419} [1 + 0.607(\Omega_m h^2)^{0.674}], \quad (84)$$

and

$$b_2 = 0.238(\Omega_m h^2)^{0.223}. \quad (85)$$

The baryon-to-photon density ratio at a given redshift is calculated as

$$R = 31.5 \Omega_m h^2 \Theta_{2.7}^{-4} \frac{1000}{z}. \quad (86)$$

The Silk damping scale is obtained using

$$k_{\text{Silk}} = 1.6(\Omega_b h^2)^{0.52} (\Omega_m h^2)^{0.73} [1 + (10.4\Omega_m h^2)^{-0.95}]. \quad (87)$$

The coefficients in the second term of the baryonic transfer function are written as

$$\alpha_b = 2.07 k_{\text{eq}} s (1 + R_d)^{-3/4} F\left(\frac{1 + z_{\text{eq}}}{1 + z_d}\right), \quad (88)$$

$$\beta_b = 0.5 + \frac{\Omega_b}{\Omega_m} + \left(3 - 2\frac{\Omega_b}{\Omega_m}\right) \sqrt{(17.2\Omega_m h^2)^2 + 1}, \quad (89)$$

where we used the function

$$F(y) = y \left[-6\sqrt{1+y} + (2+3y) \ln \frac{\sqrt{1+y}+1}{\sqrt{1+y}-1} \right]. \quad (90)$$

A shifting of nodes in the baryonic transfer function is accounted for by the quantity

$$\tilde{s}(k) = \frac{s}{[1 + (\beta_{\text{node}}/ks)^3]^{1/3}}, \quad (91)$$

where

$$\beta_{\text{node}} = 8.41(\Omega_m h^2)^{0.435}. \quad (92)$$

The symbol $\Theta_{2.7} = T/2.7$ is the temperature of the CMB relative to 2.7 K, while $h = H/(100 \text{ km/s/Mpc})$. The wave number k is in units of Mpc^{-1} .

5.2 Density fluctuations in Modified Gravity

The MOG version of the gravitational Poisson equation can be written as (see Brownstein & Moffat (2007), Eqs. 1–3, but note that in the present work, we retain the conventional factor of 4π , and maintain the sign convention of Weinberg (1972), to ensure that the source term in the perturbation equation appears in the form conventionally found in the literature):

$$\nabla \cdot \mathbf{g}(\mathbf{r}) = -4\pi G_N \rho(\mathbf{r}) - \mu^2 \Phi_Y(\mathbf{r}). \quad (93)$$

The Yukawa-like potential in this expression is

$$\Phi_Y(\mathbf{r}) = G_N \alpha \int \frac{\rho(\mathbf{r}')}{|\mathbf{r} - \mathbf{r}'|} e^{-\mu|\mathbf{r} - \mathbf{r}'|} d^3\mathbf{r}', \quad (94)$$

with α defined as in (17), such that $G_N \alpha = G_\infty - G_N$. As the initial unperturbed distribution is assumed to be homogeneous, ρ is not a function of \mathbf{r} and can be taken outside the integral sign:

$$\Phi_Y(\mathbf{r}) = G_N \alpha \rho \int \frac{1}{|\mathbf{r} - \mathbf{r}'|} e^{-\mu|\mathbf{r} - \mathbf{r}'|} d^3 \mathbf{r}'. \quad (95)$$

Varying ρ , we get

$$\nabla \cdot \delta \mathbf{g}(\mathbf{r}) = -4\pi G_N \delta \rho(\mathbf{r}) - \mu^2 G_N \alpha \delta \rho \int \frac{1}{|\mathbf{r} - \mathbf{r}'|} e^{-\mu|\mathbf{r} - \mathbf{r}'|} d^3 \mathbf{r}'. \quad (96)$$

Accordingly, (69) now reads

$$\begin{aligned} \ddot{\delta} + 2H\dot{\delta} - \frac{c_s^2}{a^2} \nabla^2 \delta - 4\pi G_N \rho \delta \\ - \mu^2 G_N \alpha \rho \delta \int \frac{e^{-\mu|\mathbf{r} - \mathbf{r}'|}}{|\mathbf{r} - \mathbf{r}'|} d^3 \mathbf{r}' = 0. \end{aligned} \quad (97)$$

The integral can be readily calculated. Assuming that $|\mathbf{r} - \mathbf{r}'|$ runs from 0 to the comoving wavelength a/k , we get

$$\begin{aligned} \int \frac{e^{-\mu|\mathbf{r} - \mathbf{r}'|}}{|\mathbf{r} - \mathbf{r}'|} d^3 \mathbf{r}' &= 2 \int_0^{a/k} \int_0^{2\pi} \int_0^{\pi/2} \frac{e^{-\mu r}}{r} r^2 \sin \theta \, dr \, d\phi \, d\theta \\ &= \frac{4\pi [1 - (1 + \mu a/k) e^{-\mu a/k}]}{\mu^2}. \end{aligned} \quad (98)$$

Substituting into (97), we get

$$\begin{aligned} \ddot{\delta} + 2H\dot{\delta} - \frac{c_s^2}{a^2} \nabla^2 \delta - 4\pi G_N \rho \delta \\ - 4\pi G_N \alpha \left[1 - \left(1 + \frac{\mu a}{k} \right) e^{-\mu a/k} \right] \rho \delta = 0, \end{aligned} \quad (99)$$

or

$$\begin{aligned} \ddot{\delta} + 2H\dot{\delta} - \frac{c_s^2}{a^2} \nabla^2 \delta \\ - 4\pi G_N \left\{ 1 + \alpha \left[1 - \left(1 + \frac{\mu a}{k} \right) e^{-\mu a/k} \right] \right\} \rho \delta = 0. \end{aligned} \quad (100)$$

This demonstrates how the effective gravitational constant

$$G_{\text{eff}} = G_N \left\{ 1 + \alpha \left[1 - \left(1 + \frac{\mu a}{k} \right) e^{-\mu a/k} \right] \right\} \quad (101)$$

depends on the wave number.

Using G_{eff} , we can express the perturbation equation as

$$\ddot{\delta}_{\mathbf{k}} + 2H\dot{\delta}_{\mathbf{k}} + \left(\frac{c_s^2 k^2}{a^2} - 4\pi G_{\text{eff}} \rho \right) \delta_{\mathbf{k}} = 0. \quad (102)$$

As the wave number k appears only in the source term

$$\left(\frac{c_s^2 k^2}{a^2} - 4\pi G_{\text{eff}} \rho \right),$$

it is easy to see that any solution of (70) is also a solution of (102), provided that k is replaced by k' in accordance with the following prescription:

$$k'^2 = k^2 + 4\pi a^2 \left(\frac{G_{\text{eff}} - G_N}{G_N} \right) \lambda_J^{-2}, \quad (103)$$

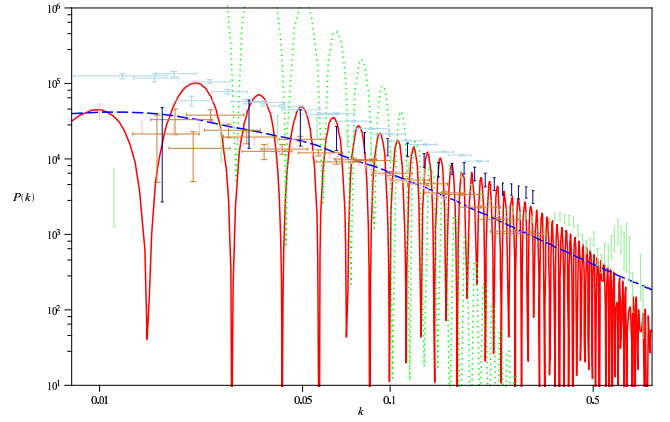


Figure 3. The mass power spectrum. Three models are compared against five data sets (see text): Λ CDM (dashed blue line, $\Omega_b = 0.035$, $\Omega_c = 0.245$, $\Omega_\Lambda = 0.72$, $H = 71$ km/s/Mpc), a baryon-only model (dotted green line, $\Omega_b = 0.035$, $H = 71$ km/s/Mpc), and MOG (solid red line, $\alpha = 19$, $\mu = 5h$ Mpc $^{-1}$, $\Omega_b = 0.035$, $H = 71$ km/s/Mpc.) Data points are colored light blue (SDSS 2006), gold (SDSS 2004), pink (2dF), light green (UKST), and dark blue (CfA).

where $\lambda_J = \sqrt{c_s^2 / G_N \rho}$ is the Jeans wavelength.

This shifting of the wave number applies to the growth term of the baryonic transfer function (76). However, as the sound horizon scale is not affected by changes in the effective gravitational constant, terms containing ks must remain unchanged. Furthermore, the Silk damping scale must also change as a result of changing gravity; as demonstrated by Padmanabhan (1993), $k_{\text{Silk}} \propto G^{3/4}$. Using these considerations, we obtain the modified baryonic transfer function

$$T_b'(k) = \left\{ \frac{\tilde{T}_0(k', 1, 1)}{1 + (ks/5.2)^2} + \frac{\alpha_b \exp(-[k/k_{\text{Silk}}]^{1.4}/G^{3/4})}{1 + (\beta_b/ks)^3} \right\} \frac{\sin k\tilde{s}}{k\tilde{s}}. \quad (104)$$

The effects of these changes can be summed up as follows. At low values of k , the transfer function is suppressed. At high values of k , where the transfer function is usually suppressed by Silk damping, the effect of this suppression is reduced. The combined result is that the tilt of the transfer function changes, such that its peaks are now approximately in agreement with data points, as seen in Figure 3.

Data points shown in this figure come from several sources. First and foremost, the two data releases of the Sloan Digital Sky Survey (SDSS) (Tegmark et al. 2004, 2006) are presented. Additionally, data from the 2dF Galaxy Redshift Survey (Cole et al. 2005), UKST (Hoyle et al. 1999), and CfA130 (Park et al. 1994) surveys are shown. Apart from normalization issues, the data from these surveys are consistent in the range of $0.01 h \text{ Mpc}^{-1} \leq k \leq 0.5 h \text{ Mpc}^{-1}$. Some surveys provide data points outside this range, but they are not in agreement with each other.

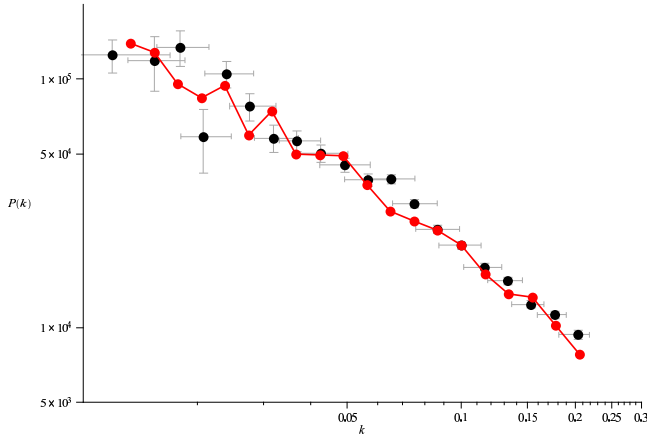


Figure 4. The effect of window functions on the power spectrum is demonstrated by applying the SDSS luminous red galaxy survey window functions to the MOG prediction. Baryonic oscillations are greatly dampened in the resulting curve (solid red line), yielding excellent agreement with the data after normalization.

5.3 Discussion

As a result of the combined effects of dampened structure growth at low values of k and reduced Silk damping at high values of k , the slope of the MOG transfer function differs significantly from the slope of the baryonic transfer function, and matches closely the observed values of the mass power spectrum. On the other hand, the predictions of MOG and Λ CDM cosmology differ in fundamental ways.

First, MOG predicts oscillations in the power spectrum, which are not smoothed out by dark matter. However, the finite size of samples and the associated window functions used to produce power spectra are likely masking any such oscillations in presently available survey data (see Fig. 4). These oscillations may be detectable in future galaxy surveys that utilize a large enough number of galaxies, and sufficiently narrow window functions in order to be sensitive to such fluctuations.

Second, MOG predicts a dampened power spectrum at both high and low values of k relative to Λ CDM. Observations at sufficiently high values of k may not be practical, as we are entering sub-galactic length scales. Low values of k are a different matter: as accurate three-dimensional information becomes available on ever more distant galaxies, power spectrum observations are likely to be extended in this direction.

In the present work, we made no attempt to account for the possibility of a non-zero neutrino mass, and its effects on the power spectrum. Given the uncertainties in the semi-analytical approximations that we utilized, such an attempt would not have been very fruitful. Future numerical work, however, must take into account the possibility of a non-negligible contribution of neutrinos to the matter density.

6 CONCLUSIONS

In this paper, we demonstrated how Modified Gravity can account for key cosmological observations using a minimum number of free parameters. Although MOG permits the running of its coupling and scaling constants with time and space, we made very little use of this fact. Throughout these calculations, we used consistently the value of $\alpha \simeq 19$ for the MOG coupling constant, consistent with a flat Einstein-de Sitter universe with $\Omega_m \simeq 0.05$ visible matter content, no dark matter, and no cosmological constant. In nearly all cosmological calculations, we set the MOG scaling constant μ to a_0^{-1} (associating a_0 with the horizon distance), which is a natural choice. The only exception is the mass power spectrum calculation, where the scaling constant enters in conjunction with the wave number k , and describes gravitational interactions between nearby concentrations of matter, not on the cosmological scale.

The theory requires *no other parameters* to obtain the remarkable fits to data that have been demonstrated here.

At all times, $\lim_{r \rightarrow 0} G = G_N$, i.e., the effective gravitational constant at very short distances remains Newton's constant of gravitation. For this reason, the predictions of MOG are *not contradicting our knowledge of the processes of the initial nucleosynthesis*, taking place at redshifts of $z \simeq 10^{10}$, since the interactions take place over distance scales that are much shorter than the horizon scale.

Our calculations relied on analytical approximations. This is dictated by necessity, not preference; we recognize that numerical methods, including high-accuracy solutions of coupled systems of differential equations, as in CMBFAST (Seljak & Zaldarriaga 1996), or N -body simulations, can provide superior results, and may indeed help either to confirm or to falsify the results presented here. Nevertheless, our present work demonstrates that at the very least, MOG provides a worthy alternative to Λ CDM cosmology.

ACKNOWLEDGMENTS

We would like to thank John Peacock for his helpful comments and suggestions. The research was partially supported by National Research Council of Canada. Research at the Perimeter Institute for Theoretical Physics is supported by the Government of Canada through NSERC and by the Province of Ontario through the Ministry of Research and Innovation (MRI).

REFERENCES

- Adelberger E. G., Heckel B. R., Nelson A. E., 2003, Annual Review of Nuclear and Particle Science, 53, 77
- Brownstein J. R., Moffat J. W., 2006a, Mon. Not. R. Astron. Soc., 367, 527
- Brownstein J. R., Moffat J. W., 2006b, Astrophys. J., 636, 721
- Brownstein J. R., Moffat J. W., 2007, to be published in Mon. Not. R. Astron. Soc.

- Cole S., Percival W. J., Peacock J. A., Norberg P. *et al.*, 2005, *Mon. Not. R. Astron. Soc.*, 362, 505
- Eisenstein D. J., Hu W., 1998, *Astrophys. J.*, 496, 605
- Fischbach E., Talmadge C., 1998, *The Search for Non-Newtonian Gravity*. Springer, AIP Press
- Goobar A., Bergström L., Mörtzell E., 2002, *A&A*, 384, 1
- Hoyle F., Baugh C. M., Shanks T., Ratchiffe A., 1999, *Mon. Not. R. Astron. Soc.*, 309, 659
- Jones W. C., Ade P. A. R., Bock J. J., Bond J. R. *et al.*, 2006, *Astrophys. J.*, 647, 823
- Moffat J. W., 1995, *Physics Letters B*, 355, 447
- Moffat J. W., 2005, *Journal of Cosmology and Astroparticle Physics*, 2005, 003
- Moffat J. W., 2006, *Journal of Cosmology and Astroparticle Physics*, 2006, 004
- Moffat J. W., 2007, To be published in *Int. J. Mod. Phys.*
- Moffat J. W., Toth V. T., 2007a, ArXiv e-prints, 0708.1935 [astro-ph]
- Moffat J. W., Toth V. T., 2007b, ArXiv e-prints, 0708.1264 [astro-ph]
- Mukhanov V., 2005, *Physical Foundations of Cosmology*. Cambridge University Press
- Padmanabhan T., 1993, *Structure formation in the universe*. Cambridge University Press
- Park C., Vogeley M. S., Geller M. J., Huchra J. P., 1994, *Astrophys. J.*, 431, 569
- Riess A. G., Strolger L.-G., Tonry J., Casertano S. *et al.*, 2004, *Astrophys. J.*, 607, 665
- Seljak U., Zaldarriaga M., 1996, *Astrophys. J.*, 469, 437
- Spergel D. N., Bean R., Doré O., Nolte M. R. *et al.*, 2007, *Astrophys. J. Suppl.*, 170, 377
- Tegmark M., Blanton M. R., Strauss M. A. *et al.*, 2004, *Astrophys. J.*, 606, 702
- Tegmark M., Eisenstein D. J., Strauss M. A. *et al.*, 2006, *Phys. Rev. D*, 74, 123507
- Weinberg S., 1972, *Gravitation and Cosmology*. John Wiley & Sons

This paper has been typeset from a \TeX / \LaTeX file prepared by the author.